CHARACTERIZATION OF THE MECHANICAL RESPONSE OF ELECTRIC ROAD PAVEMENT STRUCTURES IN HEAVY VEHICLE SIMULATOR TESTS

D. Arzjani
Ph.D. Candidate in Construction Engineering, École de Technologie Supérieure (ÉTS).

J-C. Carret
Assistant Professor, École de Technologie Supérieure (ÉTS).
Ph.D. in Civil Engineering, Université de Lyon, 2018.

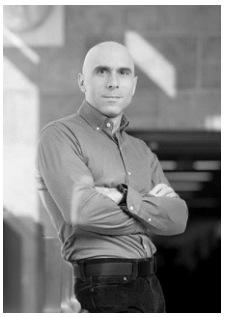

J-P. Bilodeau
Assistant Professor, Université Laval.
Ph.D. in Road Geotechnics, Université Laval, 2009.

D. Ramirez Cardona
Assistant Professor, École de Technologie Supérieure (ÉTS).
Ph.D. in Civil Engineering, Université de Lyon, 2016.

Abstract

Electric Road Systems (ERS) with wireless inductive charging technology offer a transformative solution for promoting electric vehicle (EV) adoption and reducing greenhouse gas emissions in Canada. This study investigates the mechanical behavior of asphalt pavements embedded with inductive charging coils under sustained dynamic loading, addressing a significant research gap. Three pavement structures were constructed at the Accelerated Pavement Testing (APT) facility at Laval University (Quebec, Canada): two with inductive coils beneath surface courses with thicknesses of 7 cm and 5 cm, respectively, and one conventional road structure which served as control section. Instrumented with sensors, these structures monitored vertical stress and moisture at the granular base, and strain and temperature in the asphalt layers. Using a heavy-vehicle simulator (HVS), pavements were tested under varying traffic loads (3,500, 4,500, and 5,500 kg), two water table levels, and three wheel positions to simulate real-world conditions. The results presented in this paper encompass strain and vertical stress responses at different environmental conditions.

Keywords: Pavement design, Electric Road Systems (ERS), Pavement instrumentation, Heavy Vehicle Simulator (HVS).

1. Introduction

The transition from fossil fuels to electric energy represents a critical step in mitigating global greenhouse gas emissions, particularly in the road transport sector. In Canada, transportation accounted for 28% of total greenhouse gas emissions in 2022, with road transportation alone contributing 61% (120 megatons) of this total (Environment and Climate Change Canada, 2022). Addressing emissions from road transport is thus pivotal in achieving climate goals. Electric Road Systems (ERS) have emerged as a promising solution to decarbonize transportation and reduce the reliance on fossil fuels (PIARC World Road Association, 2023).

ERS address key limitations of traditional battery storage systems, which, while effective for smaller vehicles, are less practical for heavy vehicles such as trucks and buses. Battery Electric Vehicles (BEVs) face challenges such as heavy, resource-intensive, and costly batteries, along with long recharging times. These limitations can reduce payload capacity, limit cruising range, and create congestion at charging stations. By enabling dynamic charging on the road, where vehicles receive continuous power while in motion, ERS offer a sustainable alternative that reduces battery size, lowers costs, conserves resources, and does not affect payload capacity, especially for heavy vehicles (PIARC World Road Association, 2023).

ERS technologies can be broadly classified into inductive, conductive rail, and conductive catenary systems. Inductive systems use wireless charging through coils embedded in road pavement, while conductive rail systems employ electrified rails either embedded, mounted, or positioned at the roadside. Conductive catenary systems rely on overhead electric cables, commonly used in railways.

Advancements in inductive charging have demonstrated power delivery of up to 200 kW per truck, making it a viable option for heavy-duty transport (ENRX, 2024). While 200 kW of inductive power transfer is already sufficient for many operational needs, advancements in efficiency and an increased output of up to 400 kW will further enhance the viability of inductive charging for long-distance freight transport. (Region Örebro County, 2020).

Among ERS technologies, inductive systems stand out for their seamless, contact-less charging, offering a safer and more adaptable alternative to conductive rail and catenary systems, which rely on continuous physical contact. Figure 1 illustrates the integration of inductive coils within the pavement, allowing road construction to proceed as usual.

Figure 1 – Placement of inductive charging coils in a trench and asphalt paving for inductive pavement construction (*Smartroad Gotland*, 2022)

The implementation of ERS has demonstrated significant environmental benefits. For instance, a comprehensive analysis estimates that ERS deployment could reduce CO2 emissions by up to 70% for heavy vehicles and 45% for light vehicles in countries such as Sweden and Norway (Taljegard et al., 2020). In France, full regional ERS electrification could cut emissions by 33 to 60 Mt CO2eq annually, contributing significantly to transport electrification (DGITM, 2021). While inductive charging coils offer significant potential for seamless electric vehicle charging, their integration into pavement structures requires careful evaluation to ensure long-term performance and durability. This underscores the need for further empirical studies to assess the impact of inductive systems on pavement behavior and optimize their implementation, a topic that remains largely underexplored.

A knowledge gap remains in the availability of empirical data from instrumented electrified roads (eRoads) tested under simulated or real-world traffic and environmental conditions. To bridge this gap, the "Route à recharge électrique par induction" project in Canada, supported by PRIMA Québec, examines the effects of embedding inductive charging coils in a full-scale pavement structure. This study evaluates the impact of inductive coils on pavement response and long-term performance using strategically placed instrumentation. Continuous loading tests replicate real-world traffic conditions in a laboratory environment, enabling a comparative analysis between different pavement structures, with and without embedded coils.

2. Objectives and methodology

To assess the behavior and durability of the eRoad pavement structures, a comprehensive series of tests was conducted to simulate different traffic and climate conditions, including initial response tests, freeze-thaw tests, and continuous loading tests, with a total of 946,000 equivalent single axle loads (ESAL) applied on a large-scale pavement structure with a Heavy Vehicle Simulator (HVS). This paper presents the evolution of the pavement response during continuous loading tests. Results at different stages of the tests (ESAL applied) are compared with the initial response (measured at the beginning of the tests) to evaluate the pavement's durability under repeated loadings.

To achieve the project's objectives, an indoor test pit was constructed with three distinct sections: a conventional road (tRoad) and two eRoad pavement structures containing inductive charging coils. These sections replicated the pavement designs and materials commonly used in high-traffic roadways in Quebec, Canada. These structures were subjected to simulated heavy vehicle loading under controlled temperature conditions using an HVS.

2.1 Test pit and pavement structures

The pavement structures were built within a large-scale test pit measuring 2 m in width (Y), 6 m in length (X), and 2 m in depth (Z) at Laval University's Accelerated Pavement Testing (APT) facility (see Figure 2).

The test pit comprised three sections: two eRoad pavements incorporating inductive charging coils (IS5 and IS7) and one conventional road section (CS5) without coils, serving as a reference. The CS5 and IS5 sections featured an asphalt concrete surface course of 50 mm, while section IS7's surface course was 70 mm thick. To accommodate the thicker surface course in IS7, a step was added to the granular base final grade, lowering the base course by 20 mm compared to IS5 and CS5 (Figure 2). Sections IS5 and IS7 contained inductive coils at the bottom of the surface course, while CS5 acted as the control section without coils. All sections included a 120 mm asphalt concrete base course. This design enables direct

comparisons between eRoad and tRoad structures while assessing the influence of surface course thickness.

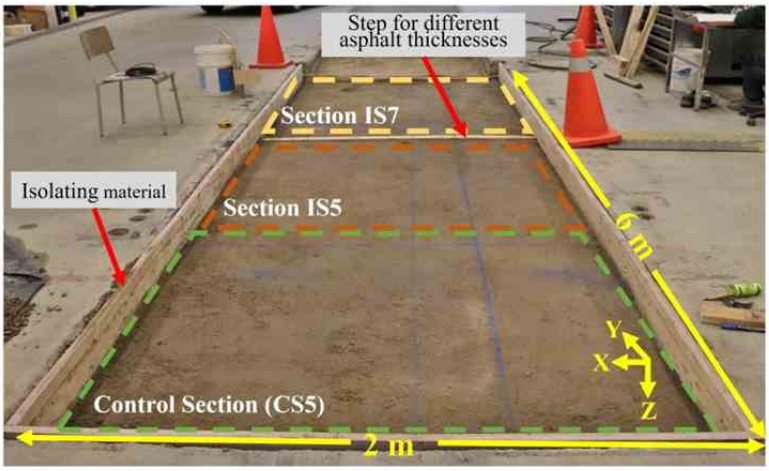

Figure 2 – Test pit at Laval university (at the final grade level of granular base layer)

2.2 Materials and instrumentation

The materials used in the test pit were characterized in accordance with the standards set by the Quebec Ministry of Transportation (*Norme 4202*, 2023). The pavement structure includes GB-20 (base course) and ESG-10 (surface course) asphalt layers with 20% reclaimed asphalt pavement (RAP) and PG 58H-34 bitumen, suited for heavily trafficked Quebec roads. The granular base and subbase are composed of MG-20 and MG-112 aggregates, with silty sand as the subgrade and clean gravel at the bottom of the test pit. A summary of pavement layers and thickness is presented in Table 1.

Table 1 - Materials and thickness of pavement layers

Layer	Material	Thickness (mm)	Depth (Z) from Surface (mm)
Surface course	ESG-10 type asphalt mix	50 or 70	0–50/70
Base course	GB-20 type asphalt mix	120	50/70–170/190
Granular Base	0/20-mm granular base (MG-20)	197 or 177	170/190–367
Granular Subbase	0/112-mm granular subbase (MG-112)	474	367–841
Subgrade (Soil)	Silty sand (SM)	859	841–1700
Clean Gravel	Crushed stone	300	1700–2000

The inductive charging coils, provided by Electreon Wireless Ltd, consist of copper wires encased in a rubber-like polymer, referred to as “rubber strips” in this study. The wires converge in a solid box, termed the “capacitor unit”, which connects them to the power grid. However, in this study, the coils remain disconnected from the grid. Using magnetic resonance induction, these coils facilitate wireless energy transfer to a receiver mounted beneath an electric vehicle (EV). Notably, the rubber strips exhibit significantly lower stiffness compared to conventional asphalt mixtures, potentially influencing the structural behavior of the pavement.

To investigate this potential impact, the test pit was equipped with sensors strategically placed throughout its structure. The details about the construction and instrumentation of the test pit are presented in a previous publication (Arzjani et al., 2024). Figure 3 presents the plan views of load cells and strain gauges at the corresponding pavement depths. Vibrating wire load cells (TPC circular model, 230 mm diameter, with ±0.5% accuracy) measured pressure levels in the granular base, while asphalt strain gauges (TML KM-100HAS, with ±1% accuracy) captured strain distribution at the bottom of the asphalt base course layer. Additionally, temperature and moisture probes monitored environmental conditions at various depths. The instrumentation positioning is schematized in Figure 4.

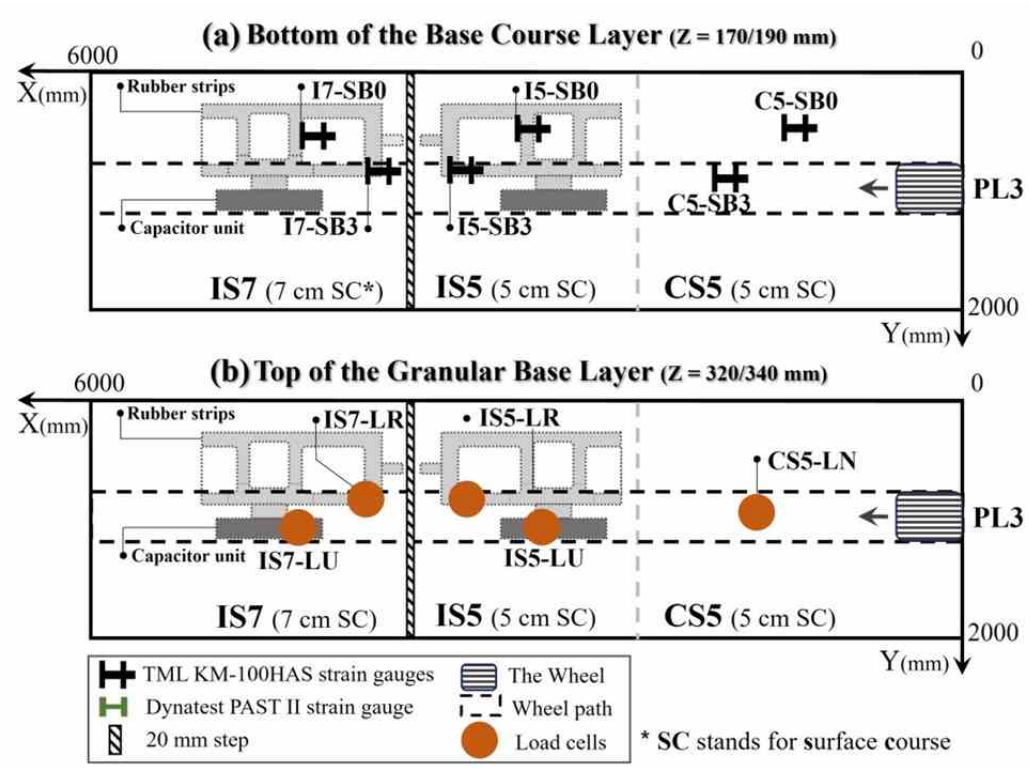

Figure 3 – Schematic of the plan views of the instrumentation of the test at Depths: (a) Z= 170–190 mm, (b) Z = 320–340 mm

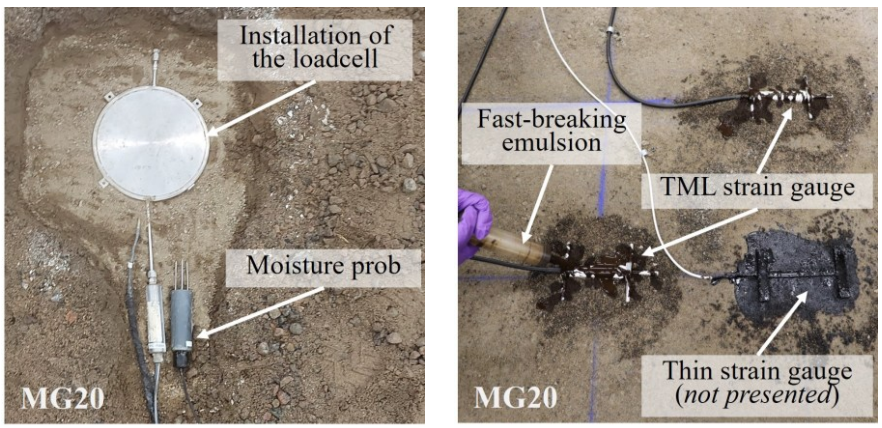

(a) **(b)**

Figure 4 – Pavement instrumentation: (a) load cells and moisture probes in the granular base layer (MG-20), (b) strain gauges at the bottom of the base course (GB-20).

2.3 HVS and wheel properties

The ATLAS Heavy Vehicle Simulator (HVS) utilized in this study (see Figure 5-a) enables full-scale accelerated pavement testing by simulating heavy traffic loads in a temperature-controlled test chamber. Equipped with advanced heating, cooling, and hydraulic systems, the HVS ensures precise temperature control within a range of -15°C to +40°C. Additionally, the system can regulate the water table and ground temperature to replicate realistic environmental conditions influencing pavement performance.

For this study, the loading carriage was configured with a 455/55R22 wide-base single tire (see Figure 5-b), widely used as a steering tire on Canadian heavy trucks. The executed test plan was designed to replicate real-world traffic conditions by incorporating a wheel wander of ±250 mm. The inflation pressure of the tire was set to 690 kPa during the tests.

(a) **(b)**

Figure 5 – ATLAS Setup: (a) HVS installed on the test pit, and (b) the tire used for traffic simulation

In pavement engineering, the reference load for a single axle with dual tires is typically 80 kN (ARA Inc, 2004). In Quebec, regulations permit a legal maximum load of 100 kN during normal periods and 80 kN during thaw periods for a rear single axle (Ministère des Transports du Québec, 2013). For a half-single axle, this corresponds to a load of 4,000 kg. When applied to a dual-tire configuration, this 4-ton load produces tire contact pressures equivalent to those of a wide-base single tire carrying 3,500 kg, as confirmed through surface contact area analysis for the tested setup.

To simulate and assess the effect of axle load, wheel loads of 3,500 kg, 4,500 kg, and 5,500 kg were applied, representing spring thaw, normal, and overload scenarios in Quebec. Three loading positions were evaluated: PL1, representing the wheel path of vehicles traveling centered in a lane during normal service life; PL2, with a lateral offset of 25 cm from PL1 placing the wheel path directly over the capacitor unit; and PL3, simulating off-center traffic such as overtaking maneuvers, with a lateral offset of 25 cm from PL2 and wheel path directly over the rubber strips. Table 2 summarizes the loading parameters and their characteristics.

Table 2 - Characteristics of the loading conditions

Parameter	Value	Unit
Carriage speed	9	Km/h
Half-single axle load	Spring thaw reduced load: *3,500* Standard load: *4,500* Overload: *5,500*	kg
Load off-set	PL1: Off-center PL2: Over capacitor unit of the coil PL3: Over the rubber strip and the capacitor unit	
Tire dimensions	455/55R22.5	–
Tire inflation pressure	690	kPa

The equivalent single-axle load (ESAL) concept is widely used across North America to evaluate pavement performance and assist in design (Kawa et al., 1998). It quantifies the damage from various axle configurations as the equivalent number of passes by a single axle with dual tires carrying 8,181 kg (18,000 lbs.). Guidelines for ESAL calculations are provided by organizations such as the Transportation Association of Canada (*TAC*, 1997) and the American Association of State Highway and Transportation Officials (*AASHTO*, 1986).

To ensure accurate assessment of pavement impacts for the tested tire type across different load conditions, a customized ESAL equation developed by FPInnovations (Bradley & Thiam, 2020), shown in Equation 1, was utilized.

$$\text{ESAL} = 5.81 - 1.12 \times L + 0.094 \times L^2 - \frac{10.2}{L} \quad (1)$$

In the equation, L represents the axle load in tons (1,000 kg). The results presented in the figures within the results and discussion section of this paper are expressed in terms of ESAL for more clarity.

2.4 Testing plan

The number of passes at each loading position (PL1, PL2 and PL3) was determined based on the probability distribution of vehicle positions reported in the literature (Gungor & Al-Qadi, 2022). Moreover, to approximate realistic axle load distribution, a lateral wander value of 25 cm was employed. This value aligns with the NCAT report, and the AASHTO MEPDG (Timm & Priest, 2005; AASHTO, 2008).

As outlined in the testing plan (Figure 6), the study consisted of three phases:

- Phase 1 consisted of 100,000 wheel passes carried out in low groundwater table (GWT) conditions (1500 mm below surface), all using the 4,500 kg load, and all loading positions (PL1, PL2 and PL3) in three steps;
- Phase 2 consisted of 100,000 passes carried out in high GWT conditions (500 mm below surface), divided into six steps, with mixed loads (4,500 and 5,500 kg) applied at all loading positions (PL1, PL2, and PL3);
- Phase 3 consisted of 100,000 passes at PL3, focusing on directly loading the inductive coils with a 5,500 kg load.

ESAL values were for each step and phase, displaying cumulative and stepwise totals at the left side of the testing plan given in Figure 6. This chart expresses the loading history of the pavement structures during this study in all loading positions. It is noteworthy that Phase 1, as

presented in this study, does not correspond to 0 ESAL, as some tests were conducted prior to the initiation of continuous loading on the pavement structures. These initial tests are referred to as the "Response tests" since they aimed at characterizing the response of the pavement structures under different load and temperature conditions. seven (7) wheel passes were applied for each test condition, resulting in a cumulative total of 24,308 ESAL prior to the commencement of Phase 1 of the "Continuous loading" treated in this paper.

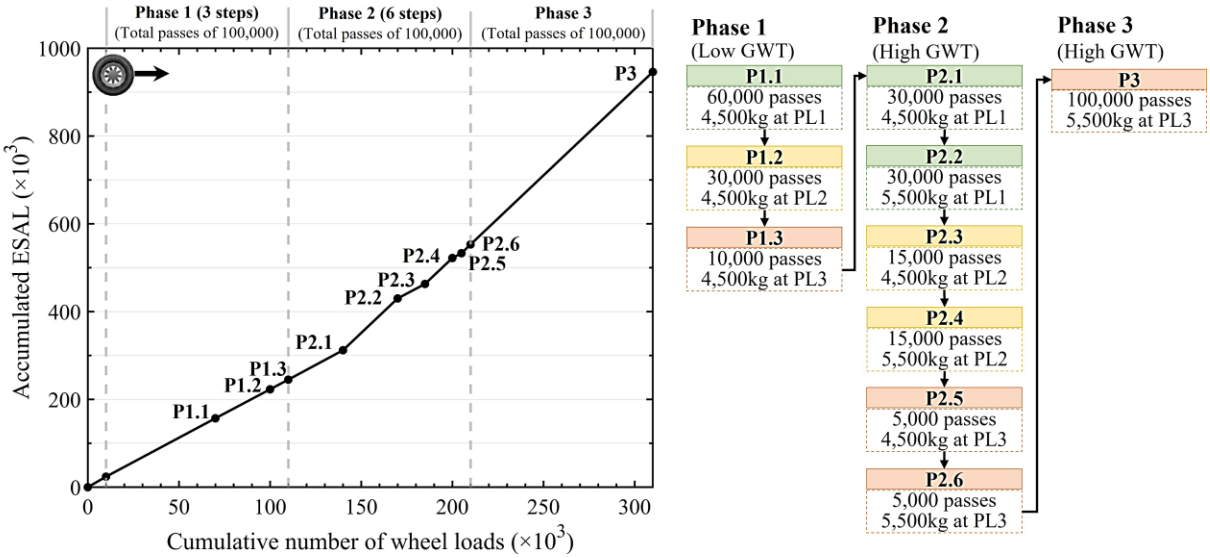

Figure 6 – Testing plan during continuous loading tests – the dots in the chart represent the beginning of each step of the 3 phases of the continuous loading testing

3. Results and discussion

3.1 Analysis approach

In the following subsections, the impact of the loading path (load position) is evaluated, focusing on the stress transferred to the top of the granular base and the strain response within the asphalt base course. Measurements across all three pavement structures (sections) are compared: control section (CS5) and the inductive sections (IS5 and IS7). Stress measurements were obtained from load cells, while strain levels were recorded using strain gauges positioned at the bottom of the asphalt base course layer.

For each measurement point, seven wheel passes were performed using the Heavy Vehicle Simulator (HVS). For each set of seven passes, the average maximum stress (termed "Maximum pressure") and the average maximum strain values—both extension and contraction (referred to collectively as "Maximum deformation")—were calculated. Standard deviation values, consistently below 2% of the mean, demonstrated excellent repeatability of the measurements at all test points for each loading condition.

For clarity in the analysis, the values that are compared in this paper correspond to those measured under the specific load configuration of 5,500 kg with high GWT. These correspond to values measured at the end of the test steps P2.2, P2.4, P2.6 and P3. Such values are compared to those from the initial response tests conducted prior to the continuous loading tests.

To track the evolution of stress and strain over time, results are presented for three key moments of the testing plan:

- Before continuous loading: A negligible number of cumulated ESAL (referred to as 0 ESAL), meaning the first time that the structures were tested at 5,500 kg and high GWT, during the response tests (serving as the baseline for comparison),
- Mid-test plan: 430,000 ESAL for PL1 and 553,000 ESAL for PL3, corresponding to the end of step P2.2 and P2.6, respectively, of the continuous loading test,
- End of the test plan: 946,000 ESAL, meaning the last time that the structures were tested at the loading conditions used for comparison, corresponding to the end of step P3.

Additionally, temperature gradients and volumetric water content within the pavement were monitored throughout the experiment. These measurements, illustrated in Figure 7, correspond to the end of the initial response tests and the continuous loading steps P2.2, P2.6 and P3.

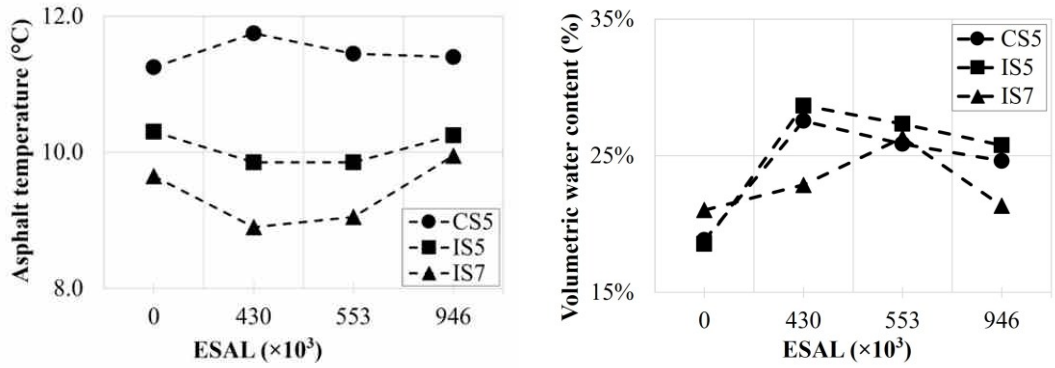

Figure 7 – Asphalt temperature and volumetric water content (in the granular base) in all sections during the loading experiments

3.2 Vertical stress at the top of the granular base

Figure 8-a depicts the signal patterns recorded by the load cells, which are positioned at the top of the granular base layer. Figure 8-b presents the maximum vertical stress values measured by load cell CS5-LN, at load positions PL1 and PL3, during continuous loading phases. Notably, the stress levels recorded at PL3 are substantially higher—up to 20 times—than those at PL1. Interestingly, a similar trend was observed in the two inductive sections, which is consistent with the principles of pavement mechanics. These principles suggest that stress transfer to the granular base is most significant directly beneath the load application point.

Regarding the stress evolution during the test plan, at PL3, situated above the inductive coils, stress levels in the inductive sections increased as the number of cumulated ESAL increased during the test, while the control section exhibited no significant changes in stress levels after 946,000 equivalent single-axle loads (ESAL).

Regarding the absolute values of stress measured at the top of the granular base when the load is in PL3 position, a comparison between the inductive and control sections revealed that the stress amplitudes measured at the top of the granular base beneath the rubber strip of the inductive coil were lower than those in the control section. This result is contrary to expectations based on the stiffness of the materials and may be attributed to adhesion deficiencies between the rubber and the asphalt layers, or to localized strain/stress concentrations near the rubber strips. However, there is no significant differences between the stress measured in either section when the load is in PL1 position. These findings underscore the localized effects introduced by the presence of inductive coils in the pavement structure.

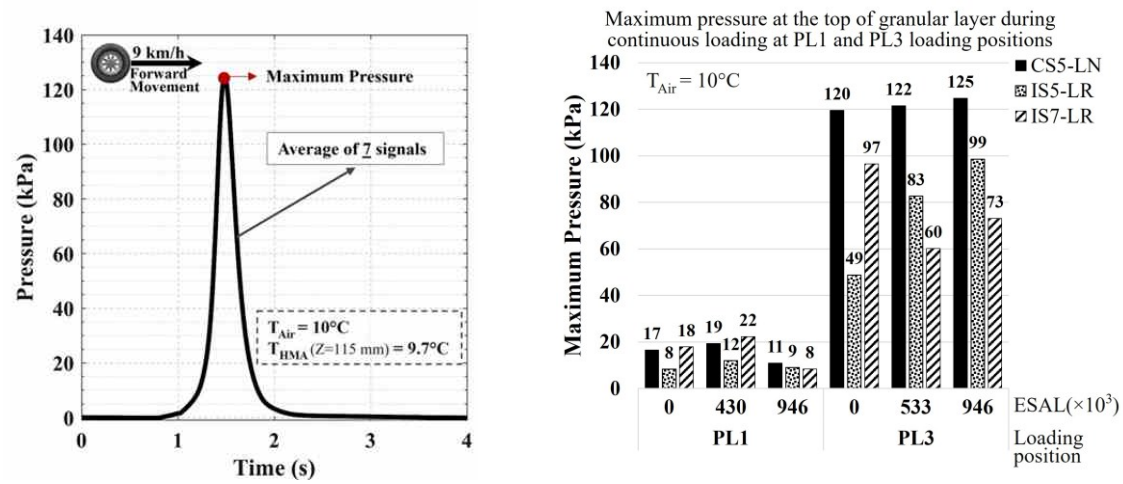

(a) **(b)**

Figure 8 – (a) Average stress signals from load cell CS5-LN, (b) Maximum stress values at PL1 and PL3 loading positions across all sections during continuous loading phases.

3.3 Strain at the bottom of the asphalt base course

Figure 9-a illustrates the longitudinal strain signal measured by sensor C5-SB3 at the bottom of the asphalt concrete base course layer (GB-20), highlighting maximum extension (ε_e) and the maximum contraction (ε_c), defined as the greater absolute value of ε_{c1} and ε_{c2}, measured before and after the wheel passes. Figure 9-b, presents maximum strain values at the bottom of the base course of the control section, recorded by C5-SB3 (under the loading path at PL3) and C5-SB0 (outside the wheel path). Results indicate that strain levels (extension and contraction) are higher under the loading path, with noticeable load effects still being noticeable by the sensor outside the load path. Nonetheless, similarly to stress values, strain levels at the PL1 loading position are significantly lower than at PL3, with minimal variation observed at PL1. During Phase 3, the on-path sensor C5-SB3 recorded an increase in extension values, from 256 microstrain at the end of Phase 2 to 317 microstrain at the end of Phase 3, reflecting a 24% rise with only 394,000 ESAL applied. This increase is likely due to the concentrated loading at the PL3 position, suggesting greater susceptibility of the areas around the coils to strain evolution.

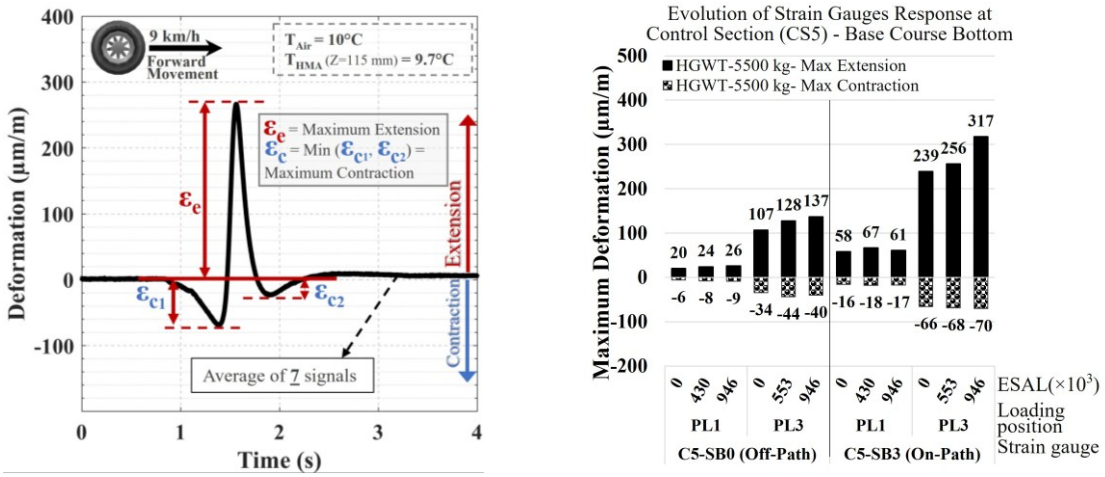

(a) **(b)**

Figure 9 – (a) Average strain signals from strain gauge C5-SB3, (b) Maximum strain values measured in control section during the evolutions of loadings

Figure 10 compares the strain levels recorded by strain gauges located under the loading path at PL3 across all sections. A comparison between the inductive section IS5 and the control section CS5 reveals minimal differences in strain variations as the number of cumulated ESAL increased at both PL1 and PL3, except for increased contraction in IS5 at the end of the tests. In contrast, section IS7, with its 2-cm thicker wearing course, exhibits greater changes as the number of cumulated ESAL increased during the test, particularly at the PL3 loading position.

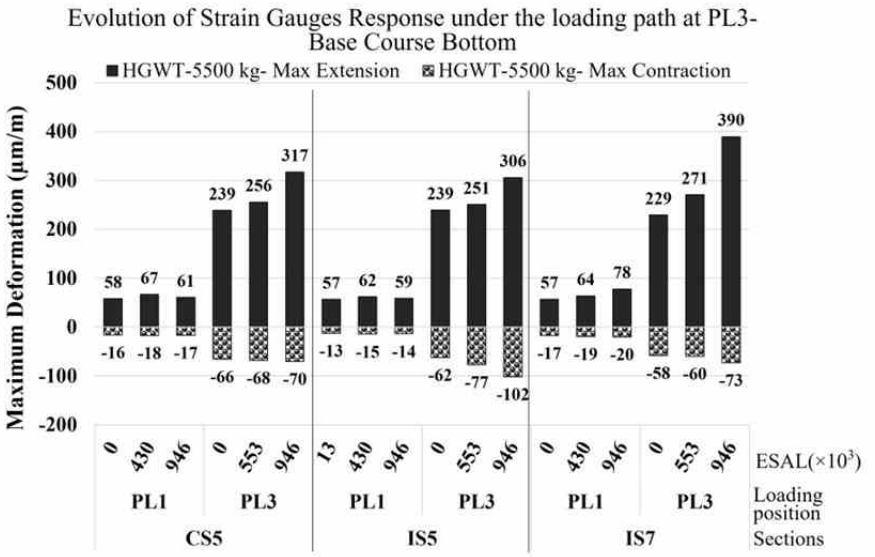

Figure 10 – Maximum strain values in all sections measured at the key moments of the test plan

The increase in stress and strain during Phase 3 of continuous loading tests suggests potential damage, observed across all test sections and is most pronounced in IS7. This observation highlights the need for further investigation into strain levels around the coil, as the coils may have localized effects on the pavement structure. To better understand the evolution of strain, future work should focus on assessing the integrity of asphalt concrete and the bonding between layers and rubber strips to better understand strain development.

4. Conclusion

This study evaluated the effects of inductive charging coils on pavement performance through large-scale laboratory testing under continuous heavy loading using a Heavy Vehicle Simulator (HVS). Three pavement configurations were tested: a conventional road structure with no inductive coils, serving as the control section, and two inductive sections with coils embedded at the bottom of the surface asphalt course. These two sections had different surface course thicknesses. Results demonstrated lower vertical stress levels at the top of the granular base directly beneath the coils, compared to those measured at the control section with no coils. It was also observed that all tested pavement structures presented a similar evolution of strain values at the bottom of the asphalt base course layer. These findings suggest that the coils have limited influence on overall pavement behavior. However, during Phase 3 of continuous loading, higher strain values were recorded when 394,000 ESAL were applied exclusively over the coils, with the IS7 section—featuring a 2 cm thicker surface course—showing the most pronounced increase. This unexpected behavior suggests localized effects near the coils, particularly under concentrated loading, which may explain the observed strain increases and highlight the need for further investigation.

5. References

- AASHTO. (2008). Mechanistic-empirical pavement design guide: A manual of practice. American Association of State Highway and Transportation Officials.
- AASHTO. (1986). Guide for Design of Pavement Structures. Washington, D.C.
- Transportation Association of Canada. (1997). Pavement Design and Management Guide. Ottawa, ON.
- Arzjani, D., Ramirez Cardona, D., Carret, J.-C., Bilodeau, J.-P., & Auger, S. (2024). *Instrumentation of a Pavement Structure Containing Inductive Charging Equipment in the Canadian Context.* In Proceedings of the Canadian Society for Civil Engineering Annual Conference 2023**,** Vol. 7, 1–14. https://doi.org/10.1007/978-3-031-61511-5_1
- Bradley, A., & Thiam, P.-M. (2020). *Development of a methodology to estimate ESALs for Widebase Steering Tires.* In Transportation Association of Canada 2020 Conference and Exhibition - The Journey to Safer Roads. https://trid.trb.org/View/1754885
- Timm, D. H., & Priest, A. L. (2005). *Wheel wander at the NCAT test track.* In Proceedings of the NCAT Test Track Conference**.** https://trid.trb.org/View/787744
- Gungor, O. E., & Al-Qadi, I. L. (2022). *Wander 2D: A flexible pavement design framework for autonomous and connected trucks.* International Journal of Sustainable Transportation, 23, 121–136. https://doi.org/10.1080/10298436.2020.1735636
- Taljegard, M., Thorson, L., Odenberger, M., & Johnsson, F. (2020). *Large-scale implementation of electric road systems: Associated costs and the impact on CO2 emissions.* International Journal of Sustainable Transportation**,** 14(8), 606–619. https://doi.org/10.1080/15568318.2019.1595227
- ARA Inc. (2004). *Guide for the Mechanistic-Empirical Design of New and Rehabilitated Pavement Structures* (Final report No. NCHRP 1-37A). Transportation Research Board of the National Academies**.**
- DGITM. (2021). *Système de route électrique: Décarboner le transport routier de marchandise par l'ERS, enjeux et stratégie* (No. 2021a). Direction générale des infrastructures, des transports et de la mer**.** https://www.ecologie.gouv.fr/sites/default/files/documents/GT1%20rapport%20final.pdf
- ENRX. (2024). *Groundbreaking 200 kW electrified roadway: ENRX, CFX, ASPIRE, Oldcastle.* https://www.enrx.com/en/Company/Media/News/ASPIRE-Electric-Roadway-test-track---Electrifying-the-future-of-transportation
- Environment and Climate Change Canada. (2022). *National Inventory Report: Greenhouse Gas Sources and Sinks in Canada.* [Electronic].
- Kawa, I., Zhang, Z., & Hudson, W. R. (1998). *Evaluation of the AASHTO 18-Kip Load Equivalency Concept* (Report No. 0-1713-1).
- Ministère des Transports du Québec. (2013). *Load and Size Limits for Road Vehicles.* Direction du transport routier des marchandises, Direction des communications**.**
- Norme 4202. (2023). *Enrobés à chaud formulés selon la méthode de formulation du Laboratoire des chaussées***.** Ministère des Transports et de la Mobilité Durable**.**
- PIARC World Road Association. (2023). *Electric Road Systems: A Route to Net Zero* (p. 187). 2023R30EN - Technical Report**.**
- Region Örebro County. (2020). *Electric road pilot E20 Hallsberg–Örebro.* https://utveckling.regionorebrolan.se/globalassets/media/dokument/regional-utveckling/samhallsplanering-och-infrastruktur/electric-road-pilot-e20-hallsberg-orebro.pdf
- Smartroad Gotland. (2022). *Smartroad Gotland Blog.* https://www.smartroadgotland.com/blog